Binding-Induced DNA Assembly and Its Application to Yoctomole Detection of Proteins

ARTICLE *in* ANALYTICAL CHEMISTRY · JANUARY 2012

Impact Factor: 5.64 · DOI: 10.1021/ac203207g · Source: PubMed

3 AUTHORS:

Hongquan Zhang
University of Alberta
35 PUBLICATIONS **1,190** CITATIONS
SEE PROFILE

Xing-Fang Li
University of Alberta
123 PUBLICATIONS **3,128** CITATIONS
SEE PROFILE

X. Chris Le
University of Alberta
248 PUBLICATIONS **7,753** CITATIONS
SEE PROFILE

analytical chemistry

Accelerated Article

pubs.acs.org/ac

Binding-Induced DNA Assembly and Its Application to Yoctomole Detection of Proteins

Hongquan Zhang,[†] Xing-Fang Li,[†] and X. Chris Le*[,†,‡]

[†]Department of Laboratory Medicine and Pathology, Faculty of Medicine and Dentistry, and [‡]Department of Chemistry, University of Alberta, 10-102 Clinical Sciences Bldg., Edmonton, Alberta, Canada T6G 2G3

Supporting Information

ABSTRACT: We describe the binding-induced DNA assembly principle and strategy that enable ultrasensitive detection of molecular targets and potential construction of unique nanostructures/nanoreactors. Two DNA motifs that are conjugated to specific affinity ligands assemble preferentially only when a specific target triggers a binding event. The binding-induced assembly of the DNA motifs results in the formation of a highly stable closed-loop structure, raising the melting temperature (T_m) of the hybrid by >30 °C and enabling effective differentiation of the target-specific assembly from the background. The ability to detect as few as a hundred molecules (yoctomole) of streptavidin, platelet derived growth factor, and prostate specific antigen represents an improvement of detection limits by 10^3−10^5-fold over traditional immunoassays. The assay is performed in a single tube, eliminating separation, immobilization, and washing steps of conventional assays. By incorporating unique signaling and structural features into the DNA motifs, we envision diverse applications in biosensing and nanotechnology.

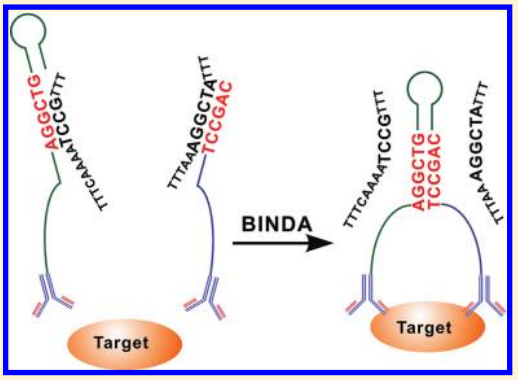

Self-assembly is one of the most common strategies for generating nanostructures, in which components spontaneously assemble into organized structures as a consequence of noncovalent interactions.[1,2] The exquisite specificity of base pairing and its remarkable structure features make DNA one of the most promising building blocks for nanotechnology. DNA nanotechnology takes advantage of DNA self-assembly to construct defined nanostructures in one, two, and three dimensions.[3−9] Distinguishing from the extensive studies on DNA self-assembly, we aim to construct a molecular assembly that depends on binding of a specific target. We term this "binding-induced DNA assembly (BINDA)" because such assembly is preferentially formed only when a specific target triggers a binding event. Potential applications of BINDA range from detection of specific target molecules to fabrication of novel nanoswitches and target-dependent nanostructures.

Achieving BINDA requires that any nonspecific DNA self-assembly is diminished, which is technically challenging. Recognizing that DNA self-assembly is dependent on the stability of the hybrid of cDNA sequences, which is governed by the concentration, length, and GC content of the complementary sequences, we focus on design principles that manipulate these critical parameters. Recent studies have demonstrated remarkable increase of local effective concentrations of complementary sequences through binding of two DNA tethered-affinity ligands to a single target molecule.[10−14] The increased local concentrations favor the hybridization of DNA sequences that would otherwise be difficult to achieve at low concentrations.[13−16] The target-induced DNA association has been applied to analysis of biomolecules, in vitro selection for bond formation, and identification of ligand−target pairs.[14,17−20]

Motivated by these previous innovations, we explore here the use of binding-induced DNA association to assemble DNA motifs with more sophisticated secondary structures and multiple components. We further hypothesize that the BINDA strategy could eliminate DNA self-assembly through rational design and control of DNA motifs. In the present study, we first considered the theoretical basis of the BINDA to determine key parameters that affect the performance of BINDA. We then combined the rational design with experimental optimization to manipulate these critical parameters. While maximizing BINDA, elimination of DNA self-assembly resulted in overcoming the background problem commonly encountered in the detection of minute amounts of molecular targets. Detection of streptavidin, platelet derived growth factor (PDGF), and prostate specific antigen (PSA) at the yoctomole to zeptomole levels, using biotin, aptamer, and antibody as affinity ligands, suggest diverse applications of the BINDA principle to many molecular targets.[21]

EXPERIMENTAL SECTION

Safety Consideration. The experiments were performed in a Level 2 certified biosafety laboratory and the usual biosafety procedures were followed.

Received: December 3, 2011
Accepted: December 20, 2011
Published: December 20, 2011

Scheme 1. Schematic Showing the General Principle of Binding-Induced DNA Assembly[a]

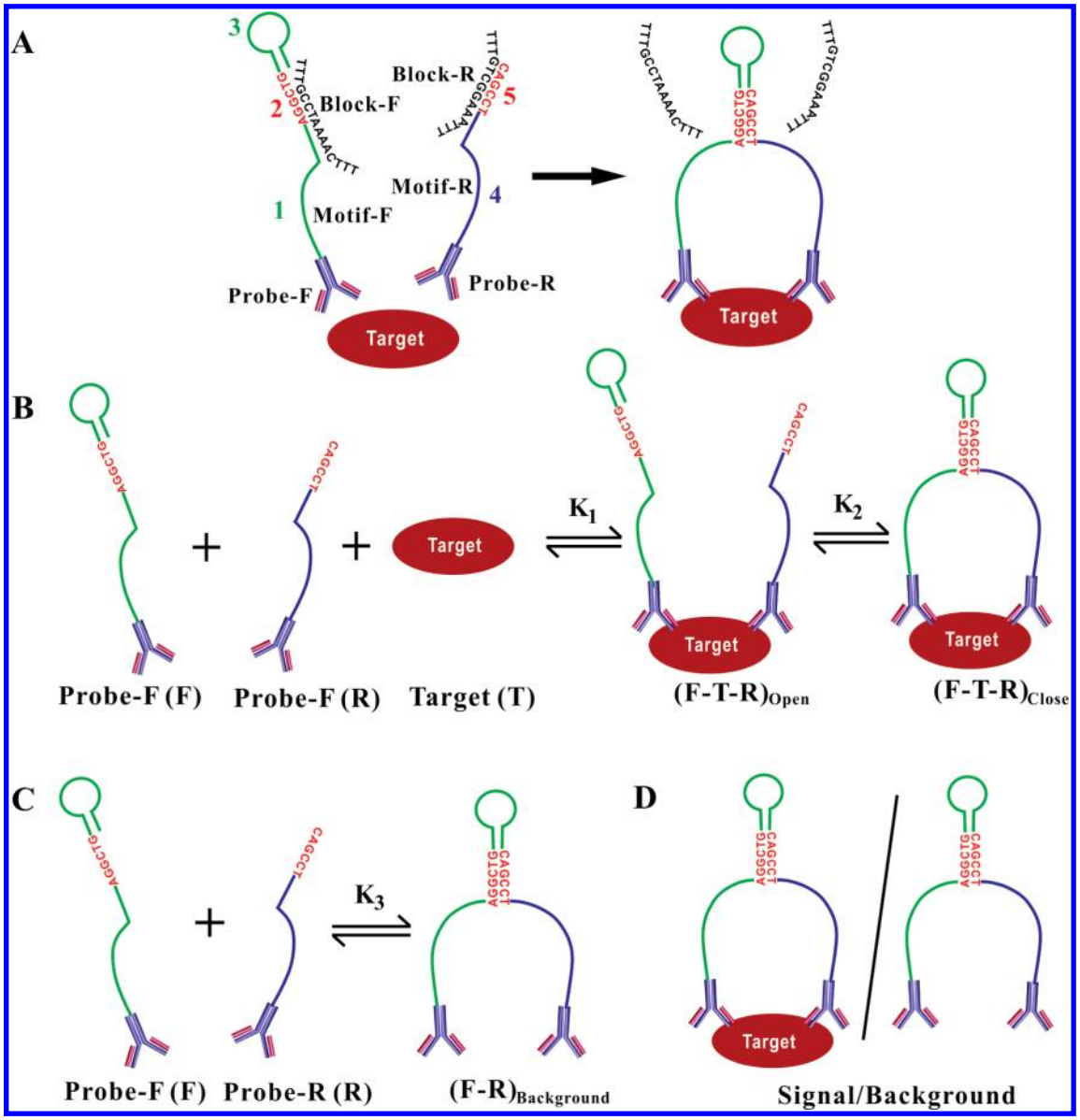

[a](A) All components involved in the formation of binding-induced DNA assembly. (B) Equilibria relating to the target, probes, and the binding-induced DNA assembly. (C) Equilibrium relating to the self-assembly. (D) Assembly corresponding to signal-to-background ratio.

Reagents. The oligonucleotides and DNA motifs (listed in Table S1 in Supporting Information) were custom synthesized, labeled, and purified by Integrated DNA Technologies (IDT, Coralville, IA). Oligo-F was conjugated to a biotin group at the 5′ end, and all forms of Oligo-R (R5, R6, R7, and R8) were biotinylated at the 3′ end. PDGF-AA, PDGF-AB, PDGF-BB, and biotinylated polyclonal anti-PSA antibody were obtained from R&D Systems (Minneapolis, MN). Streptavidin, PSA, bovine serum albumin (BSA), goat serum, and biotin were obtained from Sigma-Aldrich (Oakville, ON). SYBR GreenER qPCR Supermix Universal was obtained from Invitrogen Canada (Burlington, ON). Phosphate buffered saline (1× PBS) (137 mM NaCl, 10 mM phosphate, 2.7 mM KCl, pH 7.4) was diluted with deionized water from 10× PBS buffer (Fisher Scientific, Nepean, ON). All other reagents were of analytical grade.

Design of DNA Motifs. DNA motif-F was designed to comprise three oligonucleotides (Scheme 1, Sequences **1**, **2**, and **3**), and motif-R was designed to contain two oligonucleotides (Sequences **4** and **5**). The sequences of these DNA oligos are shown in Table S1 in Supporting Information. DNA motif-F (58 n.t. in total length) consisted of a spacing Sequence **1** (32 n.t.) that was used to link an affinity probe to Sequence **2** (8 n.t.). Sequence **2** was linked to a hairpin Sequence **3** (18 n.t.). DNA motif-R (47−50 n.t. in total length) consisted of a spacing Sequence **4** (42 n.t.) that was used to link an affinity probe to Sequence **5** (5−8 n.t.). Sequences **2** and **5** in the two DNA motifs were designed to be complementary to each other but not to hybridize to any other part of the two DNA motifs.

The design of the complementary Sequences **2** and **5** was crucial for differentiating the binding-induced DNA assembly from the background self-assembly. Devising the lengths and the GC contents of these two complementary sequences was guided by estimating the difference in the melting temperature (ΔT_m) between the hybrid of complementary Sequences **2** and **5** in the desired $(F\text{-}T\text{-}R)_{Close}$ assembly (Scheme 1B) and the

dx.doi.org/10.1021/ac203207g | Anal. Chem. 2012, 84, 877−884

corresponding hybrid in $(F\text{-}R)_{Background}$ (Scheme 1C). The goal is to have much higher T_m for the hybrid in the binding-induced assembly $(F\text{-}T\text{-}R)_{Close}$ than for the hybrid in $(F\text{-}R)_{Background}$, so that $(F\text{-}T\text{-}R)_{Close}$ is stable while $(F\text{-}R)_{Background}$ is unstable at room temperature. We used OligoAnalyzer (IDT) to estimate the T_m of the hybrid in $(F\text{-}R)_{Background}$ and in the binding-induced assembly $(F\text{-}T\text{-}R)_{Close}$. The input parameters used for these estimations were 5 nM DNA, 3 mM Mg^{2+}, and 50 mM Na^+. To estimate the T_m of the binding-induced assembly $(F\text{-}T\text{-}R)_{Close}$, a hairpin structure with a loop containing 100−130 thymidines was used. Sequence **2** was fixed as TTAGGCTG, and the tested complementary Sequence **5** varied from 5 bases (R5, CAGCC) to 6 bases (R6, CAGCCT), 7 bases (R7, CAGCCTA), and 8 bases (R8, CAGCCTAA). In all cases, the estimated T_m difference between the binding-induced assembly $(F\text{-}T\text{-}R)_{Close}$ and the self-assembled $(F\text{-}R)_{Background}$ was >30 °C. This large difference in thermal stability enabled successful formation of the binding-induced assembly while diminishing the background due to self-assembly.

The hairpin Sequence **3** was designed to facilitate enzymatic ligation of DNA motif-F and motif-R following binding-induced assembly of the two motifs. The 3′ end of the hairpin Sequence **3** was available to be linked to the 5′ end of the complementary Sequence **5** by enzymatic DNA ligation. The 5′ end of Sequence **5** was labeled with a phosphate group to facilitate the ligation. Design considerations of the hairpin Sequence **3** included: formation of a stable hairpin under experimental conditions, no hybridization to any other part of Oligo-F, and as short a sequence as possible once the first two criteria were met.

Sequences **1** and **4** were designed to provide linkages with affinity probes and to serve as spacers between the affinity complexes and the DNA motifs. To accommodate molecules of different sizes, we designed the length of spacing Sequences **1** and **4** to contain 77 nucleotides, which is equivalent to a maximum length of ∼25 nm (based on 3.3 Å per nucleotide). Within the total length of 77 n.t., Sequences **1** and **4** also contained forward or reverse primer regions to allow for the subsequent real-time PCR detection. Forward and reverse primers were evaluated using Primer Express 3.0 Software (Applied Biosystems, Foster City, CA) to avoid the formation of any undesirable byproduct. Other design considerations of Sequences **1** and **4** also included: not to form any stable secondary structure within the sequences and not to form a heterodimer between the two sequences. Formation of a heterodimer between Sequences **1** and **4** would result in target-independent assembly of the two DNA mofits and undesirable background.

Design of Blocking Oligos. Block-F and Block-R were designed to compete with the hybridization between the complementary Sequences **2** and **5**. Block-R (e.g., TTTCAAAAAGGCTGTTT) was designed to hybridize to Sequence **5** (CAGCCT) and a portion of Sequence **4** (TTTTG). Block-F (e.g., TTTGCCTAAAACAATTT) was designed to hybridize to a portion of Sequence **1** (TTGTTTT) and only 4 bases of Sequence **2** (AGGC). By this careful design, Block-F and Block-R have only 4 complementary bases, avoiding any potential hybridization between Block-F and Block-R. Therefore, much higher concentrations (1000-fold higher than the affinity probes) of the two blocking oligos were used to prevent the formation of $(F\text{-}R)_{Background}$, blocking the nontarget hybridization between Sequences **2** and **5**. As an additional consideration, Block-F and Block-R were designed to contain three noncomplementary thymines at both their 3′ and 5′ ends, further preventing the formation of potential PCR byproduct from these oligonucleotides.

Sequences of Block-R6 were used when Probe-R was constructed from Oligo-R6, while sequences of Block-R7 were used when Probe-R was constructed from Oligo-R7. Underlined sequences of Block-F and Block-R are complementary to the corresponding underlined sequences in Oligo-F and Oligo-R, respectively.

Experimental Optimization of DNA Motifs Using Streptavidin as a Target. Determination of streptavidin was used as a model system to optimize the various design and experimental parameters. The overall objective of the optimization experiments was to achieve maximum signal-to-background ratio. Oligo-F was biotinylated at the 5′ end, serving as Probe-F. Oligo-R6 (or R5, R7, R8) was biotinylated at the 3′ end, serving as Probe-R. Binding of streptavidin to the two biotinylated probes resulted in the formation of the binding-induced DNA assembly.

Optimization of the length and GC content of complementary Sequences 2 and 5 was carried out by comparing the performances of different pairs of Probe-F and Probe-R for analysis of 0.1 pM (10^{-13} M) streptavidin. Four different sample solutions (50 μL) were prepared in 1× phosphate buffered saline (PBS) and 0.2% BSA. Each final solution contained 0.1 pM streptavidin, 100 pM Oligo-F, and 100 pM Oligo-R (R5, R6, R7, or R8). Four corresponding blank solutions (50 μL) that contained all the reagents but not streptavidin were analyzed under the same conditions as for the samples, and the analyses of these blank solutions provided information on the magnitude of background. Sample and blank solutions were incubated at 37 °C for 30 min and then at room temperature for another 10 min. A 2-μL aliquot of each incubation solution was used for DNA enzymatic ligation and real-time PCR detection. Difference in threshold cycle (ΔC) between each sample and its corresponding blank solution was used to evaluate signal-to-background ratio.

To optimize the sequences for Block-F and Block-R, four sample solutions (50 μL each) were prepared in 1× PBS buffer containing 0.2% BSA. Each sample solution contained 0.1 pM streptavidin, 100 pM Oligo-F, 100 pM Oligo-R6, and 100 nM blocking oligo pairs (Block-F1 and Block-R6-1, Block-F2 and Block-R6-3, Block-F3 and Block-R6-3, or Block-F4 and Block-R6-4). Four corresponding blank solutions (50 μL) were prepared to test the background. These blank solutions contained all the above reagents but not streptavidin. After incubation at 37 °C for 30 min and room temperature for another 10 min, 2 μL of each solution was subjected to DNA enzymatic ligation and real-time PCR detection.

The concentrations of Probe-F and Probe-R were optimized by analyzing 0.1 pM streptavidin and blank in solutions containing different concentrations of Probe-F and Probe-R6. These solutions in 1× PBS buffer contained 0.2% BSA, 100 nM Block-F5, 100 nM Block-R6-4, varying concentrations (5 pM, 20 pM, 100 pM, or 500 pM) of Probe-F and Probe-R6, and either the absence (blank) or the presence (sample) of 0.1 pM streptavidin.

Analysis of Platelet Derived Growth Factor. To prepare probes for analysis of PDGF-BB, 100 μL of 400 nM Oligo-F was mixed with 100 μL of 200 nM streptavidin in 1× PBS to link Oligo-F to streptavidin in one vial. In a separate vial, 100 μL of 400 nM Oligo-R was mixed with 100 μL of 200 nM

dx.doi.org/10.1021/ac203207g | Anal. Chem. 2012, 84, 877−884

streptavidin in 1× PBS to link Oligo-R to streptavidin. After incubation at 37 °C for 1 h, 100 μL of each of the above solutions was then added to 100 μL of 100 nM biotinylated aptamer in 1× PBS. The mixture was incubated at 37 °C for another 1 h, forming Probe-F and Probe-R, respectively. The Probe-F and Probe-R solutions were each diluted to 10 nM in 1× PBS buffer containing 1% BSA and 1 mM biotin and stored at 4 °C.

Because the same DNA motifs were used for detection of streptavidin, the optimization of parameters was focused on comparison of the performances of probes with six or seven complementary bases in the presence of various pairs of Block-F and Block-R. PDGF-BB was measured in 1× PBS and in cell lysate. Different amounts of PDGF-BB were incubated with 100 pM aptamer probes (F and R), 100 nM Block-F4, and 100 nM Block-R6-4, in either 1× PBS with 0.2% BSA or cell lysate. $MgCl_2$ (1 mM) was also added to assist the formation of aptamer in its preferred secondary structure. After incubation at 37 °C for 30 min and room temperature for another 10 min, 2 μL of the incubation solution was used for subsequent DNA enzymatic ligation and real-time PCR detection.

Analysis of Prostate Specific Antigen. To prepare probes for analysis of PSA, linking Oligo-F or Oligo-R to streptavidin was first carried out by incubation of 100 μL of 400 nM Oligo-F or Oligo-R with 200 nM streptavidin in 1× PBS at 37 °C for 1 h. The above solution (100 μL) was then added to 100 μL of 100 nM biotinylated polyclonal anti-PSA antibody (R&D Systems) in 1× PBS. After incubation at room temperature for another 1 h to form Probe-F or Probe-R, the Probe-F or Probe-R solution was then diluted to 10 nM in 1× PBS buffer containing 1% BSA and 1 mM biotin and stored at 4 °C.

Similar to analysis of PDGF-BB, the optimization of parameters was focused on comparison of performances of probes with six or seven complementary bases in the presence of various pairs of Block-F and Block-R. PSA was measured in 1× PBS or in diluted goat serum. Different amounts of PSA were incubated with 100 pM Probe-F and Probe-R7 and 100 nM Block-F4 and Block-R7-4 in 1 × PBS with 0.2% BSA or diluted goat serum. After incubation at 37 °C for 30 min and room temperature for another 10 min, 2 μL of the incubation solution was subjected to subsequent DNA enzymatic ligation and real-time PCR detection.

Enzymatic Ligation of DNA. To detect the binding-induced assembly, we introduced an enzymatic ligation step to join Sequences **3** and **5**, facilitating the subsequent real-time PCR amplification and detection of the specific sequence. The ligation time could affect both background and signals from the assembly. To evaluate the ligation time on the signal-to-background, a sample solution was prepared in 1× PBS buffer containing 0.1 pM streptavidin, 100 pM Oligo-F, 100 pM Oligo-R6, 100 nM Block-F4, 100 nM Block-R6-4, and 0.2% BSA. A corresponding blank solution was prepared in the same manner except without streptavidin. Both sample and blank solutions were each split into four aliquots. Four pairs of sample and blank aliquots were subjected to different enzymatic ligation time (5 min, 10 min, 20 min, or 30 min). For the determination of 10^{-13} M streptavidin, 10 min of ligation time provided the optimum signal-to-background ratio.

Real-Time PCR. DNA enzymatic ligation and real-time PCR were carried out in a single tube. A 2 μL aliquot of the sample solutions for analysis was transferred into a 96-well real-time PCR plate (Applied Biosystems). To the well were added the reagents for ligation and PCR amplification, making the final volume 20 μL for each reaction solution that contained 100 μM ATP, 0.4 Unit T4 DNA ligase (Invitrogen, Burlington, ON), 0.1 μM primers (forward and reverse), ROX reference dye, 10 μL of SYBR GreenER qPCR SuperMix Universal (Invitrogen), and 0.2% BSA. Unless otherwise indicated, the plate was placed at room temperature for 10 min to allow for ligation reaction. The plate was then loaded onto a real-time PCR instrument (7500 Fast Real-Time PCR System, Applied Biosystems). The temperature cycle program for the real-time PCR consisted of 50 °C for 2 min and 95 °C for 10 min, followed by 50 cycles of 95 °C for 15 s and 60 °C for 60 s.

Cell Lysate. Approximately, 2 × 10^6 Vero 76 monkey kidney cells in 1.5 mL of medium were spun at 2000*g* for 3 min. The cell pellet was washed three times with cold 1× PBS and was then resuspended in 250 μL of ice-cold lysis buffer containing 20 mM Tris (pH 7.4), 150 mM NaCl, 0.1% Triton, 1 μg/mL leupeptin, and 0.5 mM PMSF. The freeze and thaw method was used for cell lysis. The lysate was centrifuged at 15 000*g* for 10 min at 4 °C. The supernatant was transferred to another tube and diluted 2-fold with 1× PBS containing 2 mM $MgCl_2$. The cell lysate was either analyzed immediately or stored at 4 °C until analysis.

Goat Serum. The frozen goat serum (Sigma-Aldrich) was thawed in a water bath at 30 °C and then kept on ice. Prior to analysis, 0.5 mL of serum was centrifuged at 10 000 rpm for 10 min, and the supernatant was used for the subsequent analysis. To prepare for samples with supplemented PSA, appropriate amounts of a PSA stock solution were added to 2.0 μL serum, and each mixture was diluted with 1× PBS to a final volume of 50 μL.

RESULTS AND DISCUSSION

General Principle of BINDA. To demonstrate the general principle of BINDA, we first designed two DNA motifs that are each conjugated to an affinity probe recognizing the target molecule (Scheme 1). Each of the two DNA motifs has a short complementary sequence (8 n.t. in Sequence **2** and 5−8 n.t. in Sequence **5**), rendering the self-assembly between the two strands unstable (T_m < 10 °C). Binding of the two affinity probes to the same target molecule results in the stable assembly of the DNA motifs for two main reasons: (i) the dramatically increased local concentrations of the DNA motifs and (ii) the formation of the closed loop structure involving the target and DNA motifs. DNA motif-F (58 n.t. in total length, Table S1 in Supporting Information) consists of a spacing Sequence **1** (32 n.t.) that links the affinity Probe-F to the complementary Sequence **2** (8 n.t.). Sequence **2** is linked to a hairpin Sequence **3** (18 n.t.) and is partially hybridized to Block-F that is designed to further minimize the nondesirable target-independent DNA self-assembly. DNA motif-R (47−50 n.t. in total length) consists of a spacing Sequence **4** (42 n.t.) that links the affinity Probe-R to the complementary Sequence **5** (5−8 n.t.). Sequence **5** is partially hybridized to Block-R that is designed to reduce the background from potential target-independent hybridization between Sequences **2** and **5**. To achieve binding-induced DNA assembly, motif-F and motif-R assemble through hybridization of complementary Sequences **2** and **5** only when both Probe-F and Probe-R bind to a single target molecule. The assembly of the two motifs brings the 3′ end of the hairpin Sequence **3** next to the 5′ end of complementary Sequence **5**. The binding-induced assembly comprising the target molecule linked to the DNA motifs

dx.doi.org/10.1021/ac203207g | *Anal. Chem.* 2012, 84, 877−884

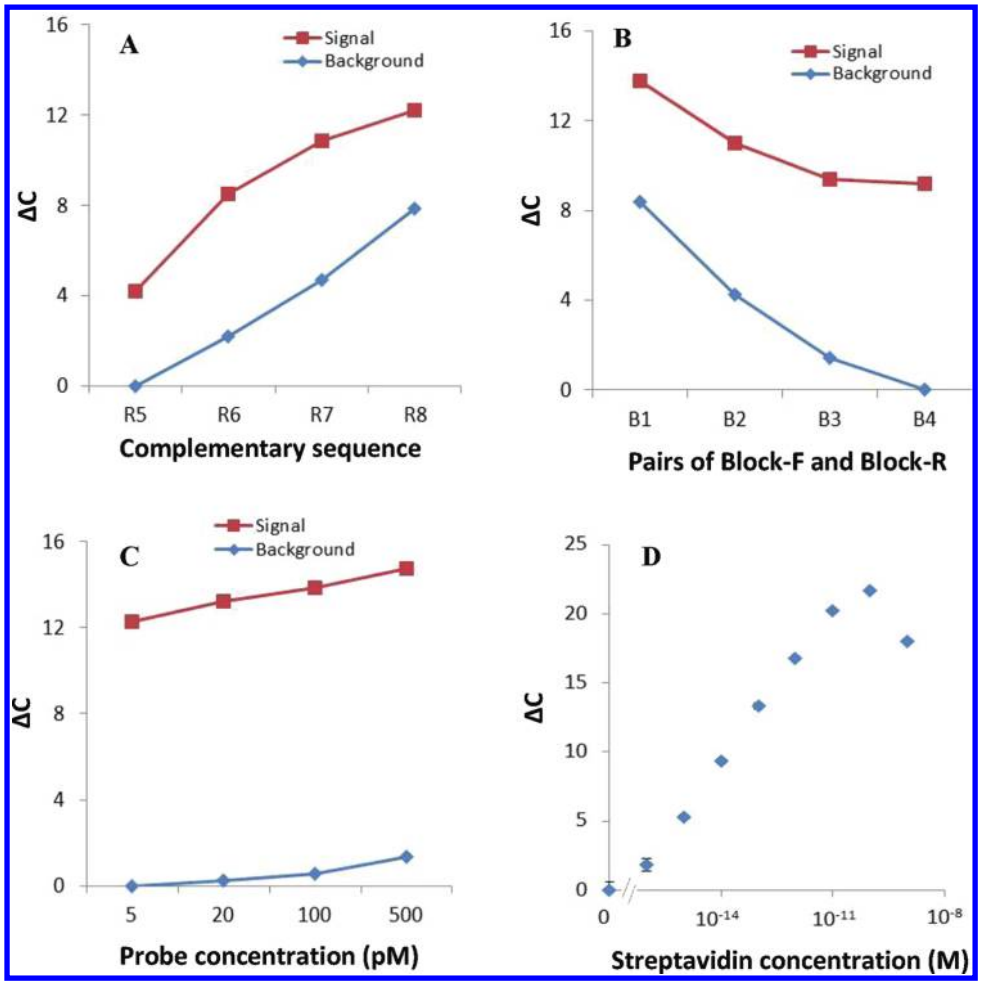

Figure 1. Results showing key design parameters that influence the binding-induced DNA assembly (signal) and the nonspecific self-assembly (background). (A) Clear differentiation between signal and background when Sequence **5** (R5, R6, R7, and R8) containing 5−8 complementary bases (see Table S1 in Supporting Information) with Sequence **2** was used. (B) Increasing the length of the blocking sequences resulted in decreased background. The pair B4 (Block-F4 and Block-R6-4) with 11 blocking bases exhibited the highest signal-to-background. Other pairs were B1 (Block-F-1and Block-R6-1), B2 (Block-F-2 and Block-R6-2), and B3 (Block-F-3 and Block-R6-3) (see Table S1 in Supporting Information). (C) Effect of probe concentration (Probe-F and Probe-R) on signal and background. (D) Analysis of streptavidin over wide range of concentrations (10^{-16}–10^{-9} M). The results were obtained from real-time PCR analysis and ΔC denotes net threshold cycles obtained from real-time PCR analysis. The reason for the decrease in ΔC value when streptavidin concentration is greater than 1×10^{-10} M is because the concentration of the probes (100 pM or 10^{-10} M) is insufficient to provide two molecules to bind to each streptavidin molecule. Increasing the concentrations of the probes would extend the upper range for detection of higher concentrations of streptavidin.

(Scheme 1A) can be detected using various techniques. In this study, we use enzymatic DNA ligation to join the small hairpin Sequence **3** together with Sequence **5**. We then detect the new DNA sequence using real-time PCR.

The process and key parameters involved in the binding-induced DNA assembly may be expressed in the following equations.

$$\mathrm{F} + \mathrm{R} + \mathrm{T} \overset{K_1}{\rightleftharpoons} (\mathrm{F\text{-}T\text{-}R})_{\mathrm{Open}} \overset{K_2}{\rightleftharpoons} (\mathrm{F\text{-}T\text{-}R})_{\mathrm{Close}} \quad (1)$$

where F and R are two affinity probes, T is the target molecule, $(\mathrm{F\text{-}T\text{-}R})_{\mathrm{Open}}$ is the complex in an open configuration, $(\mathrm{F\text{-}T\text{-}R})_{\mathrm{Close}}$ is the desired complex in the form of binding-induced assembly, and K_1 and K_2 are equilibrium constants (Scheme 1B).

In the absence of the target, any self-assembly of motif-F and motif-R would produce background (Scheme 1C).

$$\mathrm{F} + \mathrm{R} \overset{K_3}{\rightleftharpoons} (\mathrm{F\text{-}R})_{\mathrm{Background}} \quad (2)$$

where K_3 is equilibrium constant and $(\mathrm{F\text{-}R})_{\mathrm{Background}}$ is due to hybridization between Sequences **2** and **5** in the two DNA motifs.

The signal-to-background ratio can be expressed as follows (Scheme 1D):

$$\begin{aligned} &\mathrm{signal/background} \\ &= \frac{(\mathrm{F\text{-}T\text{-}R})_{\mathrm{Close}}}{(\mathrm{F\text{-}R})_{\mathrm{Background}}} \\ &= \frac{K_1 K_2 [\mathrm{T}]}{K_3} \\ &= \frac{\mathrm{T}_0}{K_3[\mathrm{F}][\mathrm{R}] + \frac{K_3}{K_2}[\mathrm{F}][\mathrm{R}] + \frac{K_3}{K_1 K_2}} \end{aligned} \quad (3)$$

dx.doi.org/10.1021/ac203207g | *Anal. Chem.* 2012, 84, 877−884

where T_0 is the initial concentration of the target and [F] and [R] are concentrations of free Probe-F and Probe-R, respectively. Therefore, the signal-to-background ratio is proportional to the initial concentration of the target and the equilibrium constants K_1 and K_2 and is inversely proportional to K_3 and the concentrations of the free Probe-F and Probe-R.

K_1 is dependent mainly on the binding affinity of the probes to the target, and the probes with higher binding affinity are preferred. K_2 and K_3 depend on the hybridization and thus the length and GC content of the complementary Sequences **2** and **5**. While K_2 reflects the intramolecular interaction, K_3 relates to the intermolecular hybridization of complementary Sequences **2** and **5**. The binding of the two affinity probes to the specific target brings the two complementary sequences to close proximity and dramatically increases their local effective concentrations,[8] favoring the hybridization within the same molecule more than between the molecules (K_2 much greater than K_3).

Assembly Induced by Binding Streptavidin to Biotin. To experimentally test the concept and evaluate the design principle, we initially chose the streptavidin–biotin binding system (Figure S1 in Supporting Information) for two main reasons. First, streptavidin and biotin are subsequently used throughout as universal linkers to conjugate to other affinity probes (antibodies and aptamers) for diverse applications of the BINDA strategy. Second, the strong binding between streptavidin and biotin ($K_d \sim 10^{-14}$ M) ensures a desirably large K_1,[22] thereby simplifying the design by focusing on other key parameters.

The length and GC content of complementary Sequences **2** and **5** were designed to maximize the K_2/K_3 ratio, by achieving a much higher T_m for the hybrid in the binding-induced assembly $(\text{F-T-R})_{\text{Close}}$ than for the hybrid in $(\text{F-R})_{\text{Background}}$. With the six complementary bases (R6, CAGCCT), the difference in melting temperature (ΔT_m) between the binding-induced assembly $(\text{F-T-R})_{\text{Close}}$ (T_m = 37.4 °C) and the self-assembled $(\text{F-R})_{\text{Background}}$ (T_m < 5 °C) was more than 32 °C. Thus, the binding-induced assembly $(\text{F-T-R})_{\text{Close}}$ was stable while $(\text{F-R})_{\text{Background}}$ was unstable at room temperature, resulting in excellent signal-to-background ratio (Figure 1A).

To further improve the signal-to-background ratio, we introduced Block-F and Block-R to compete with the hybridization between Sequences **2** and **5**. Block-R (e.g., TTTCAAAAAGGCTGTTT) was designed to hybridize to Sequence **5** (CAGCCT) and a portion of Sequence **4** (TTTTG). Block-F (e.g., TTTGCCTAAAACAATTT) was designed to hybridize to a portion of Sequence **1** (TTGTTTT) and only 4 bases of Sequence **2** (AGGC). Thus, Block-F and Block-R have only 4 complementary bases, avoiding any potential hybridization between them. Therefore, much higher concentrations (1000-fold higher than the affinity probes) of the two blocking oligos were used to prevent the formation of $(\text{F-R})_{\text{Background}}$. Figure 1B shows excellent signal-to-background using a pair of blocking oligos containing 11 blocking bases.

The signal-to-background ratio also depends on the concentrations of the affinity probes (F and R) as depicted in eq 3. The increase in probe concentrations enhances the formation of the binding-induced assembly (F-T-R) as expected from eq 1, but it also leads to undesirable hybridization between the two motifs, forming $(\text{F-R})_{\text{Background}}$ (eq 2). Therefore, the optimum concentrations of the two affinity probes can be experimentally determined (Figure 1C). The maximum signal-to-background was achieved using 20–100 pM probes for the detection of 10^{-13} M (100 fM) streptavidin.

To demonstrate the application of the BINDA approach, we examined the ability to form binding-induced assembly from ultralow levels of target while preventing background from target-independent DNA self-assembly. Analysis of solutions containing varying concentrations of streptavidin (1×10^{-16} M to 1×10^{-9} M) shows a linear dynamic range of over 5 orders of magnitude (1×10^{-16} M to 1×10^{-11} M) (Figure 1D). The reason for the decrease in ΔC value when streptavidin concentration is greater than 1×10^{-10} M is because the concentration of the probes (100 pM or 10^{-10} M) is insufficient to provide two molecules to bind to each streptavidin molecule. A detection limit, defined as the concentration equivalent to three times the standard deviation of the background level, was 5×10^{-17} M. This detection limit represents the ability to measure as few as 60 streptavidin molecules (100 yoctomole in 2 μL solution). The background (requiring 40.2 ± 0.9 threshold cycles to be detectable) is negligible compared to the signal from 10 DNA molecules. These results demonstrate a unique advantage of the BINDA approach in diminishing any target independent DNA self-assembly.

Binding-Induced DNA Assembly Assays for Detection of Platelet Derived Growth Factor and Prostate Specific Antigen. We further hypothesize that the same approach can be generally applicable to ultrasensitive detection of other targets. We show here two examples, one using an aptamer as the affinity ligand for PDGF-BB and the other using an antibody as an affinity ligand for PSA.

Since first reported,[23−25] aptamers have been widely utilized to develop various bioassays.[26−31] To detect PDGF, we use a specific aptamer to bind to the B chain of PDGF.[32] The biotinylated aptamer was linked through streptavidin to the biotinylated Oligo-F, forming Probe-F. In a separate preparation, the biotinylated aptamer was linked through streptavidin to the biotinylated Oligo-R, forming Probe-R. Although aptamers can be extended directly with additional nucleotides, the approach using biotin–streptavidin chemistry offer two advantages. The streptavidin not only work as a connector but also serve as a spacer that could reduce potential effects of extended oligos on the secondary conformation of the aptamer. The use of two shorter oligos also made their synthesis easier than having to prepare a longer oligo. Binding of two aptamer probes to PDGF-BB induces the formation of the assembly (Figure S2 in Supporting Information). This binding-induced DNA assembly is then detected with DNA ligation and real-time PCR amplification.

Because the same DNA motifs are used as for detection of streptavidin, the same design principle applies and the parameters can be similarly optimized. Analysis of 10^{-15}–10^{-9} M PDGF-BB, both in PBS buffer and in cell lysate, shows a linear dynamic range of over 4 orders of magnitude (1×10^{-15} M to 1×10^{-11} M) (Figure 2). The detection limit was 10^{-15} M or 1200 PDGF-BB molecules (2 zeptomole). Recognizing that the chosen aptamer binds only to the B chain, not to the A chain of PDGF,[32] we reasoned that PDGF-BB isomer can be differentiated from the PDGF-AB and PDGF-AA isomers because the AB and AA isomers cannot form the BINDA (Figure S3 in Supporting Information). Our results confirm the critical role of BINDA in highly sensitive detection and differentiation of the target from nontarget.

To detect PSA, binding of two antibody molecules to the same PSA molecule facilitates the assembly (Figure S4 in

dx.doi.org/10.1021/ac203207g | Anal. Chem. 2012, 84, 877–884

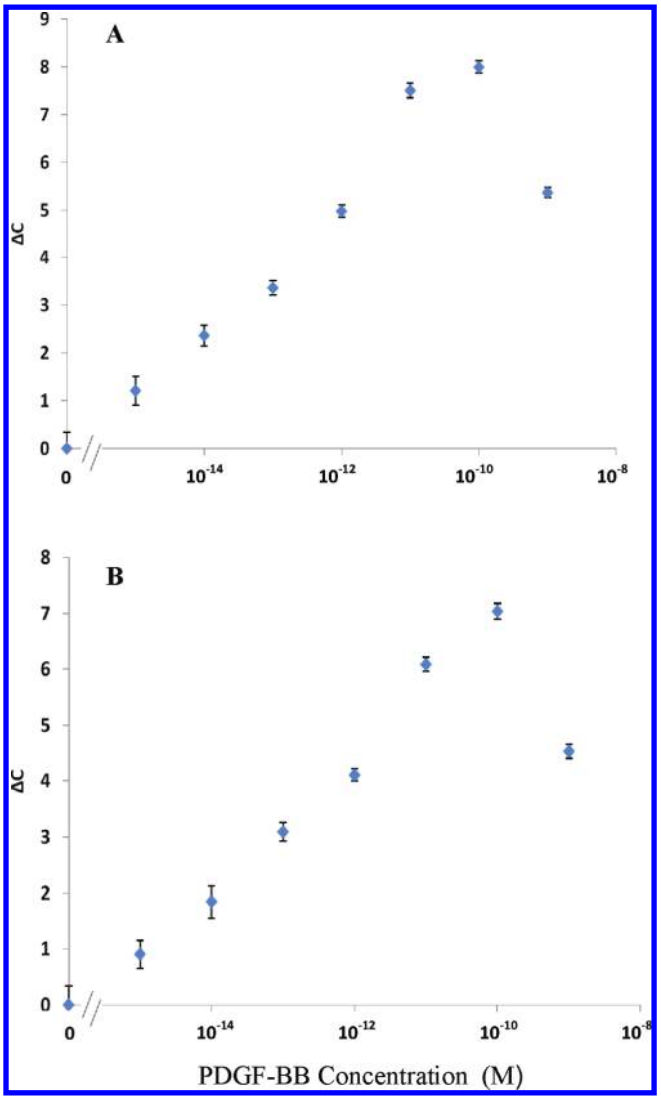

Figure 2. Analysis of PDGF-BB (10^{-16}–10^{-9} M) in PBS buffer (A) and in cell lysate (B) using the BINDA assay.

Supporting Information). The preparation of probes for analysis of PSA was similar to that for analysis of PDGF-BB. A polyclonal antibody recognizing PSA was biotinylated. One biotinylated antibody was linked to Oligo-F, forming Probe-F. Another biotinylated antibody was linked to Oligo-R6, forming Probe-R. Binding of the two probes to PSA resulted in the formation of the BINDA. This BINDA is then detected with DNA ligation and real-time PCR amplification. Analysis of PSA in standard solution and in diluted goat serum samples spiked with varying concentrations of PSA (10^{-16}–10^{-9} M) demonstrates the ability to detect as few as 120 PSA molecules or 10^{-16} M in 2 μL solution (200 yoctomole) (Figure 3).

CONCLUSIONS

The BINDA assay described here is conducted in a single tube, without need of separation, immobilization, or washing steps common to other conventional assays. The applications of the system to streptavidin, PDGF-BB, and PSA demonstrate its ability to detect yoctomole to zeptomole levels of the specific proteins in homogeneous solution, which represented an improvement of detection limits by 10^3–10^5-fold over traditional immunoassays for specific proteins.[33,34] A distinct

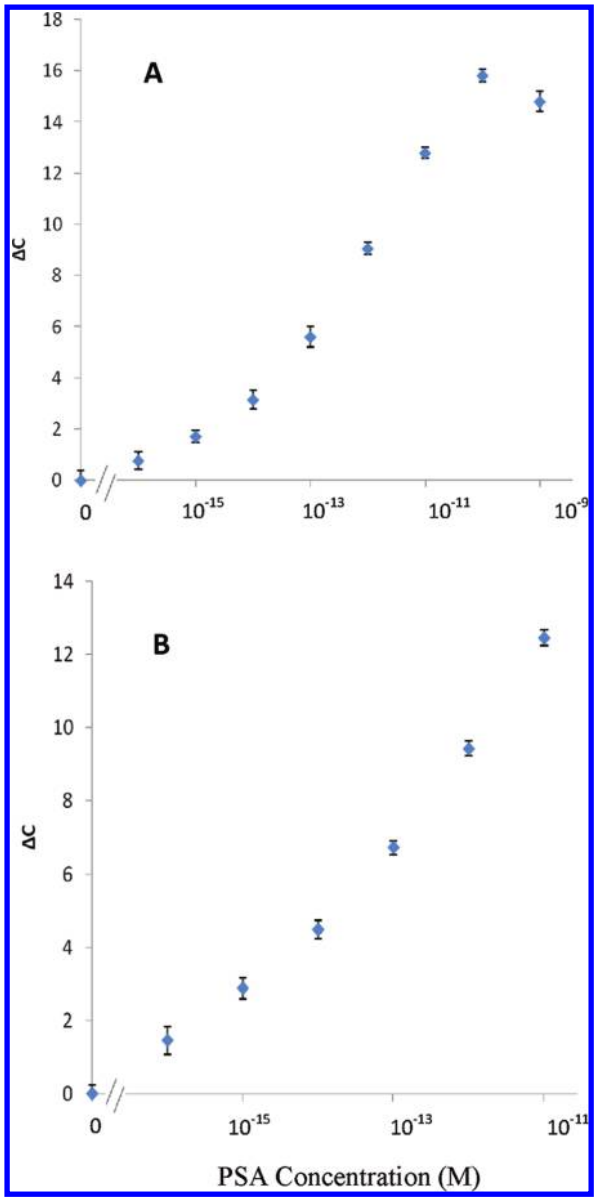

Figure 3. Analysis of PSA in PBS buffer (A) and in goat serum (B) using the BINDA assay.

advantage of BINDA through its rational design of DNA motifs is the greatly enhanced stability of BINDA, raising T_m of the hybrid by >30 °C compared to the background hybridization. Taking advantage of diminishing DNA self-assembly while maximizing binding-induced DNA assembly, we have effectively overcome the problem of background commonly encountered in the detection of minute amounts of molecular targets. The concept of BINDA can be applied to other DNA motifs and nanomaterials functionalized with DNA. The approach can be extended to any other target molecules or events capable of bringing two or more DNA motif-containing probes into close proximity (typically in the nanometer range). The principle of the BINDA strategy could potentially be used to assemble unique nanostructures, construct nanoswitches, and build nanoreactors, by incorporating unique signaling and/or structural features into the probes and DNA motifs.

dx.doi.org/10.1021/ac203207g | *Anal. Chem.* 2012, 84, 877–884

■ ASSOCIATED CONTENT

Supporting Information

Experimental details and supporting materials. This material is available free of charge via the Internet at http://pubs.acs.org.

■ AUTHOR INFORMATION

Corresponding Author

*E-mail: xc.le@ualberta.ca.

■ ACKNOWLEDGMENTS

The authors acknowledge the financial support from the Canadian Institutes of Health Research, the Natural Sciences and Engineering Research Council of Canada, the Canada Research Chairs Program, and Alberta Health and Wellness. The authors thank Mr. Feng Li for help with drawing a schematic.

■ REFERENCES

(1) Lehn, J.-M. *Angew. Chem., Int. Ed.* **1988**, *27*, 89−112.
(2) Whitesides, G. M.; Boncheva, M. *Proc. Natl. Acad. Sci. U. S. A.* **2002**, *99*, 4769−4774.
(3) Seeman, N. C. *Annu. Rev. Biochem.* **2010**, *79*, 65−87.
(4) Aldaye, F. A.; Palmer, A. L.; Sleiman, H. F. *Science* **2008**, *321*, 1795−1799.
(5) Rothemund, P. W. K. *Nature* **2006**, *440*, 297−302.
(6) Jones, M. R.; Macfarlane, R. J.; Lee, B.; Zhang, J.; Young, K. L.; Senesi, A. J.; Mirkin, C. A. *Nat. Mater.* **2010**, *9*, 913−917.
(7) Wickham, S. F.; Endo, M.; Katsuda, Y.; Hidaka, K.; Bath, J.; Sugiyama, H.; Turberfield, A. J. *Nat. Nanotechnol.* **2011**, *6*, 166−169.
(8) Macfarlane, R. J.; Lee, B.; Jones, M. R.; Harris, N.; Schatz, G. C.; Mirkin, C. A. *Science* **2011**, *334*, 204−208.
(9) Lee, J. H.; Wong, N. Y.; Tan, L. H.; Wang, Z.; Lu, Y. *J. Am. Chem. Soc.* **2010**, *132*, 8906−8908.
(10) Fredriksson, S.; Gullberg, M.; Jarvius, J.; Olsson, C.; Pietras, K.; Gústafsdóttir, S. M.; Ostman, A.; Landegren, U. *Nat. Biotechnol.* **2002**, *20*, 473−477.
(11) Söderberg, O.; Gullberg, M.; Jarvius, M.; Ridderstråle, K.; Leuchowius, K. J.; Jarvius, J.; Wester, K.; Hydbring, P.; Bahram, F.; Larsson, L. G.; Landegren, U. *Nat. Methods* **2006**, *3*, 995−1000.
(12) Schallmeiner, E.; Oksanen, E.; Ericsson, O.; Spångberg, L.; Eriksson, S.; Stenman, U. H.; Pettersson, K.; Landegren, U. *Nat. Methods* **2007**, *4*, 135−137.
(13) Heyduk, E.; Heyduk, T. *Anal. Chem.* **2005**, *77*, 1147−1156.
(14) Gorin, D. J.; Kamlet, A. S.; Liu, D. R. *J. Am. Chem. Soc.* **2009**, *131*, 9189−9191.
(15) Heyduk, E.; Dummit, B.; Chang, Y. H.; Heyduk, T. *Anal. Chem.* **2008**, *80*, 5152−5159.
(16) Di Giusto, D. A.; Wlassoff, W. A.; Gooding, J. J.; Messerle, B. A.; King, G. C. *Nucleic Acids Res.* **2005**, *33*, e64.
(17) Heyduk, T. *Biophys. Chem.* **2010**, *151*, 91−95.
(18) Blokzijl, A.; Friedman, M.; Pontén, F.; Landegren, U. *J. Intern. Med.* **2010**, *268*, 232−245.
(19) Lundberg, M.; Eriksson, A.; Tran, B.; Assarsson, E.; Fredriksson, S. *Nucleic Acids Res.* **2011**, *39*, e102.
(20) McGregor, L. M.; Gorin, D. J.; Dumelin, C. E.; Liu, D. R. *J. Am. Chem. Soc.* **2010**, *132*, 15522−15524.
(21) Le, X. C.; Zhang, H.; Li, X.−F. United States patent application US 61/238,368. Filed on August 31, 2009. PCT WO 2011/022820 A1.
(22) Green, N. M. *Methods Enzymol.* **1990**, *184*, 51−67.
(23) Tuerk, C.; Gold, L. *Science* **1990**, *249*, 505−510.
(24) Ellington, A. D.; Szostak, J. W. *Nature* **1990**, *346*, 818−822.
(25) Gold, L.; Polisky, B.; Uhlenbeck, O.; Yarus, M. *Annu. Rev. Biochem.* **1995**, *64*, 763−797.
(26) Liu, J.; Cao, Z.; Lu, Y. *Chem. Rev.* **2009**, *109*, 1948−1998.
(27) German, I.; Buchanan, D. D.; Kennedy, R. T. *Anal. Chem.* **1998**, *70*, 4540−4545.
(28) Kostal, V.; Katzenmeyer, J.; Arriaga, E. A. *Anal. Chem.* **2008**, *80*, 4533−4550.
(29) Cella, L. N.; Sanchez, P.; Zhong, W.; Myung, N. V.; Chen, W.; Mulchandani, A. *Anal. Chem.* **2010**, *82*, 2042−2047.
(30) Li, J.; Xu, M.; Huang, H.; Zhou, J.; Abdel-Halimb, E. S.; Zhang, J. R.; Zhu, J. J. *Talanta* **2011**, *85*, 2113−2120.
(31) Zhang, H.; Li, X. F.; Le, X. C. *J. Am. Chem. Soc.* **2008**, *130*, 34−35.
(32) Green, L. S.; Jellinek, D.; Jenison, R.; Ostman, A.; Heldin, C. H.; Janjic, N. *Biochemistry* **1996**, *35*, 14413−14424.
(33) Rosi, N. L.; Mirkin, C. A. *Chem. Rev.* **2005**, *105*, 1547−1562.
(34) Giljohann, D. A.; Mirkin, C. A. *Nature* **2009**, *462*, 461−464.